Cramér-Rao Lower Bounds for Angular Parameters Estimates from Incoherently Distributed Signals Generated by Noncircular Sources

Sonia Ben Hassen
Electronic Systems and Communication Networks Engineering
Tunisia Polytechnic School
La Marsa, Tunisia
Email: sonia.benhassen@yahoo.fr

Faouzi Bellili, Abdelaziz Samet, and Sofiène Affes
INRS-EMT
Montreal, Qc, H5A 1K6, Canada
Email: bellili@emt.inrs.ca, samet@emt.inrs.ca, affes@emt.inrs.ca

***Abstract*—In this paper, we derive for the first time analytical expressions for the stochastic Cramér-Rao lower bound (CRLB or CRB) of the angular parameters (central DOAs and angular spreads) estimates from incoherently distributed (ID) signals generated by *noncircular* sources. The new CRBs of the angular parameters are compared to those obtained from *circular* ID signals. The CRB of the central DOAs, however, are compared to those obtained from both *circular* and *noncircular* point sources. It will be shown that the CRB of both the central DOAs and the angular spreads obtained assuming *noncircular* ID sources are lower than those obtained using *circular* ID sources. This illustrates the potential gain that the noncircularity characteristic of the sources provides for the estimation of the angular parameters, especially in presence of different sources' distributions and for high angular spreads. Finally, the CRBs derived assuming *noncircular* ID signals decrease as the noncircularity rate increases. Furthermore, this decrease is more prominent at low DOA separations where the CRBs are sensitive to the noncircularity phase separation.**

Keywords: Angular parameters estimation, incoherently distributed sources, noncircularity of the signals, stochastic Cramér-Rao lower bound (CRLB).

I. Introduction

Direction of arrival (DOA) estimation for multiple plane waves impinging on an arbitrary array of sensors has received much attention, over the last several decades. In this context, many DOA estimators have been studied assuming different data models. The most commonly considered system model in array signal processing is the point source model. A class of DOA estimation methods has been developed assuming point source modeling [1]-[3]. However, in real surroundings, especially in modern wireless communication systems, local scattering in the source vicinity causes angular spreading. This more realistic signal model is called spatially distributed source model. Depending on the nature of scattering, there are two different classifications of the distributed sources in the literature: coherently and incoherently distributed (CD and ID) sources [4]. The assumption of uncorrelated ID sources has been shown to be relevant in wireless communication environments with a high base station [5]. Therefore, many algorithms have been developed considering this assumption [6]-[8].

Whatever the considered system model, the performance of any estimator is often assessed by computing and plotting its bias and variance as a function of the true SNR values. In this context, a given unbiased estimator is usually said to outperform another one, over a given SNR range, if it has a lower variance. In signal processing practices, a well-known common lower bound for the variance of unbiased estimators of a given parameter is the so-called Cramér-Rao Lower Bound (CRLB or CRB) [9]. There are two major categories of CRBs according to the statistical characteristics of transmitted signals: deterministic and stochastic. Despite the simplicity of its derivation, the deterministic CRB is known to be not achievable in practice. Hence, there has been always interest in deriving the stochastic CRB which can be asymptotically achieved by the stochastic ML estimator. In fact, an explicit expression of the stochastic DOA CRB was derived for real Gaussian distributions in [10]. This work was extended to *circular* complex Gaussian distributions for both temporally-uncorrelated and -correlated signals in [11, 12]. All the aforementioned CRBs present some practical limitations in the real world. In fact, they are mainly developed assuming point sources. Therefore, recently, the work of [13] considered a more realistic model assuming the signals to be *circular* and incoherently distributed and the CRBs of the angular parameters (the central DOAs and the angular spreads) have been successfully derived. Yet, *noncircular* complex signals are frequently encountered in digital communications. Therefore, more recently, explicit expressions for the stochastic DOA CRBs of both temporally-uncorrelated and -correlated signals generated from *noncircular* Gaussian point sources have been also derived in [14] and [15], respectively. But, to the best of our knowledge, no contributions have dealt yet with the derivation of the CRBs of the angular parameters assuming the signals to be generated from *noncircular* and incoherently distributed sources which is exactly the main focus of this paper.

This paper is organized as follows. In Section II, we introduce the system model. In Section III, an explicit expression for the considered CRB will be derived. Simulation results will be analyzed in Section IV and, finally, some concluding remarks will be drawn out.

Throughout this paper, matrices and vectors are represented by bold upper-case and bold lower-case characters, respectively. Vectors are, by default, in column orientation, while $(.)^*$, $(.)^T$ and $(.)^H$ refer to conjugate, transpose and conjugate transpose operators, respectively. Moreover, tr(.),diag(.) and $\frac{\partial .}{\partial .}$ stand for the trace, diagonal and first partial derivative operators,

978-1-4673-6555-0/15/$31.00 ©2015 IEEE

respectively, while, $\odot$ represents the Hadamard-Schur product operator. Finally, $\boldsymbol{I}_p$ and $\boldsymbol{0}_{p\times q}$ stand for the $(p \times p)$ identity matrix and the $(p \times q)$ null matrix, respectively.

II. System Model

Consider a uniform linear array of L identical sensors receiving the signals scattered from K distributed narrowband far-field sources. The output of the lth array sensor can then be modelled as a complex signal as follows for $l = 1, 2, \cdots, L$ [6-8]:

$$x_l(t) = \sum_{k=1}^{K} \int_{-\pi/2}^{\pi/2} a_l(\theta) s_k(\theta, \boldsymbol{\psi}_k, t) d\theta + n_l(t), \quad (1)$$

in which $a_l(\theta)$ is the response of the lth sensor to the unit energy source emitting from direction θ. Moreover, $s_k(\theta, \boldsymbol{\psi}_k, t)$ is the angular signal distribution of the kth source that is parameterized by the location parameter vector containing usually the central DOA $\bar{\theta}_k$ and the angular spread Δ_k of the kth source, i.e. $\boldsymbol{\psi}_k = [\bar{\theta}_k, \Delta_k]^T$. $\bar{\theta}_k$ is its *central* DOA defined as the mass center of the corresponding angular power density as follows:

$$\bar{\theta}_k = \int_{-\pi/2}^{\pi/2} \theta \rho_k(\theta, \boldsymbol{\psi}_k) d\theta, \quad (2)$$

with $\rho_k(\theta, \boldsymbol{\psi}_k)$ is the *normalized angular power density* of the kth source satisfying $\int_{-\pi/2}^{\pi/2} \rho_k(\theta, \boldsymbol{\psi}_k) d\theta = 1, \quad k = 1, 2, \ldots, K$. Moreover, Δ_k represents the maximum deviation of θ from $\bar{\theta}_k$. Its expression that is function of the standard deviation σ_k of the kth source depends on the source angular distribution. σ_k is defined as follows:

$$\sigma_k^2 = \int_{-\pi/2}^{\pi/2} (\theta - \bar{\theta}_k)^2 \rho_k(\theta, \boldsymbol{\psi}_k) d\theta. \quad (3)$$

Then, The location parameter vector $\boldsymbol{\psi}_k$ can be also written as $\boldsymbol{\psi}_k = [\bar{\theta}_k, \sigma_k]^T$, containing the angular parameters of the kth source: the central DOA and the standard deviation. In the literature, the Gaussian and Uniform shapes are the most used models for the angular distribution of sources. For these angular distributions, we have:

$$\Delta_k^{\text{Gauss}} = \sigma_k^{\text{Gauss}}, \quad (4)$$

$$\Delta_k^{\text{Unif}} = \sqrt{3}\sigma_k^{\text{Unif}}. \quad (5)$$

In this paper, we consider as angular spread the standard deviation σ_k. Finally, $n_l(t)$ stands for a zero-mean, *circular* Gaussian-distributed, spatially- and temporally-white noise at the lth sensor. Stacking the data received data over the L sensors, a time instant t, in a vector $\boldsymbol{x}(t) = [x_1(t), \ldots, x_L(t)]^T$, it follows from (1) that:

$$\boldsymbol{x}(t) = \sum_{k=1}^{K} \int_{-\pi/2}^{\pi/2} \boldsymbol{a}(\theta) s_k(\theta, \boldsymbol{\psi}_k, t) d\theta + \boldsymbol{n}(t), \quad (6)$$

where $\boldsymbol{a}(\theta) = [a_1(\theta), \ldots, a_L(\theta)]^T$ and $\boldsymbol{n}(t) = [n_1(t), \ldots, n_L(t)]^T$ are the array response and noise vectors, respectively. We also define the *conjugated* angular cross-correlation kernel of the kth and k'th sources arriving at the array from directions θ and θ' as follows:

$$p_{kk'}(\theta, \theta'; \boldsymbol{\psi}_k, \boldsymbol{\psi}_{k'}) = \mathrm{E}\{s_k(\theta, \boldsymbol{\psi}_k, t) s_{k'}^*(\theta', \boldsymbol{\psi}_{k'}, t)\}. \quad (7)$$

Recall here that we consider in this paper the ID source model. Therefore, for each source, the components arriving from different scatterers are uncorrelated. Moreover, we assume that all the distributed sources are mutually uncorrelated. Thus, (7) can be written as follows:

$$p_{kk'}(\theta, \theta'; \boldsymbol{\psi}_k, \boldsymbol{\psi}_{k'}) = \sigma_{s_k}^2 \rho_k(\theta, \boldsymbol{\psi}_k) \delta(\theta - \theta') \delta_{kk'}, \quad (8)$$

where $\sigma_{s_k}^2$ is the power of the kth source, $\delta(\theta - \theta')$ is the Dirac delta-function and $\delta_{kk'}$ is the Kronecker delta. Recall also that we consider the case of *noncircular* sources. Therefore, to handle the noncircularity, we define in the same way the *unconjugated* angular cross-correlation kernel as follows:

$$\begin{aligned} p'_{kk'}(\theta, \theta'; \boldsymbol{\psi}_k, \boldsymbol{\psi}_{k'}) &= \mathrm{E}\{s_k(\theta, \boldsymbol{\psi}_k, t) s_{k'}(\theta', \boldsymbol{\psi}_{k'}, t)\}, \\ &= \sigma_{s_k}^2 \gamma_k e^{j\phi_k} \rho_k(\theta, \boldsymbol{\psi}_k) \delta(\theta - \theta') \delta_{kk'}. \end{aligned} \quad (9)$$

where γ_k is the noncircularity rate of the kth source satisfying $0 \leq \gamma_k \leq 1$ and ϕ_k is its noncircularity phase. Now, since the sources' signals and noise components are uncorrelated, then from (6) and using (8) and (9), we prove that the *conjugated* and *unconjugated* covariance matrices of $\boldsymbol{x}(t)$, which are defined, respectively, as $\boldsymbol{R}_{xx} = \mathrm{E}\{\boldsymbol{x}(t)\boldsymbol{x}^H(t)\}$ and $\boldsymbol{R}'_{xx} = \mathrm{E}\{\boldsymbol{x}(t)\boldsymbol{x}^T(t)\}$, can be written as follows:

$$\boldsymbol{R}_{xx} = \sum_{k=1}^{K} \sigma_{s_k}^2 \boldsymbol{R}_s^{(k)}(\boldsymbol{\psi}_k) + \sigma_n^2 \boldsymbol{I}_L, \quad (10)$$

$$\boldsymbol{R}'_{xx} = \sum_{k=1}^{K} \sigma_{s_k}^2 \gamma_k e^{j\phi_k} \boldsymbol{R}'^{(k)}_s(\boldsymbol{\psi}_k), \quad (11)$$

where σ_n^2 is the unknown noise power. Moreover, $\boldsymbol{R}_s^{(k)}(\boldsymbol{\psi}_k)$ and $\boldsymbol{R}'^{(k)}_s(\boldsymbol{\psi}_k)$ represent, respectively, the normalized *conjugated* and *unconjugated* noise-free covariance matrices corresponding to the kth source. They are given by

$$\boldsymbol{R}_s^{(k)}(\boldsymbol{\psi}_k) = \int_{-\pi/2}^{\pi/2} \rho_k(\theta, \boldsymbol{\psi}_k) \boldsymbol{a}(\theta) \boldsymbol{a}^H(\theta) d\theta, \quad (12)$$

$$\boldsymbol{R}'^{(k)}_s(\boldsymbol{\psi}_k) = \int_{-\pi/2}^{\pi/2} \rho_k(\theta, \boldsymbol{\psi}_k) \boldsymbol{a}(\theta) \boldsymbol{a}^T(\theta) d\theta. \quad (13)$$

III. Derivation of the CRB for noncircular Gaussian distributed signals generated from ID sources

In this section, we assume that the transmitted signals $\{\boldsymbol{s}(t)\}_{t=1,2,\ldots,N}$ are zero-mean Gaussian distributed and generated from *noncircular* ID sources. To take advantage of the signal noncircularity, we define the extended received vector as follows:

$$\widetilde{\boldsymbol{x}}(t) = \left(\begin{array}{cc} \boldsymbol{x}(t), & \boldsymbol{x}^*(t) \end{array} \right)^T. \quad (14)$$

Then, the extended covariance matrix can be written as:

$$\boldsymbol{R}_{\widetilde{x}\widetilde{x}} = \mathrm{E}\{\widetilde{\boldsymbol{x}}(t)\widetilde{\boldsymbol{x}}^H(t)\} = \left(\begin{array}{cc} \boldsymbol{R}_{xx} & \boldsymbol{R}'_{xx} \\ \boldsymbol{R}'^*_{xx} & \boldsymbol{R}^*_{xx} \end{array} \right), \quad (15)$$

where $\boldsymbol{R}_{xx}$ and $\boldsymbol{R}'_{xx}$ are defined in (10) and (11), respectively. As stated earlier, we consider in this paper the Gaussian and Uniform shapes. Moreover, we assume small angular spreads. This hypothesis is practical especially in suburban areas and macro-cell environments [16]. Considering this assumption, it

was shown in [17] that the normalized conjugated noise-free covariance matrix $\boldsymbol{R}_s^{(k)}(\boldsymbol{\psi}_k)$ can be written as:

$$\boldsymbol{R}_s^{(k)}(\boldsymbol{\psi}_k) = \boldsymbol{a}(\bar{\theta}_k)\boldsymbol{a}^H(\bar{\theta}_k) \odot \boldsymbol{T}(\boldsymbol{\psi}_k) = \boldsymbol{\Phi}(\bar{\theta}_k)\boldsymbol{T}(\boldsymbol{\psi}_k)\boldsymbol{\Phi}^H(\bar{\theta}_k), \tag{16}$$

where $\boldsymbol{\Phi}(\bar{\theta}_k) = \text{diag}(\boldsymbol{a}(\bar{\theta}_k))$. Moreover, $\boldsymbol{T}(\boldsymbol{\psi}_k)$ is a $(L \times L)$ real-valued symmetric Toeplitz matrix. It depends on the nature of the angular distribution of the sources [17] as follows:

$$[\boldsymbol{T}]_{pl}^{\text{Gauss}}(\boldsymbol{\psi}_k) = \exp\left(-\frac{1}{2}\left(\tfrac{2(p-l)\pi d}{\lambda}\sigma_k\cos(\bar{\theta}_k)\right)^2\right), \tag{17}$$

$$[\boldsymbol{T}]_{pl}^{\text{Unif}}(\boldsymbol{\psi}_k) = \text{sinc}\left(\sqrt{3}\tfrac{2(p-l)\pi d}{\lambda}\sigma_k\cos(\bar{\theta}_k)\right), \tag{18}$$

with d standing for the distance between two successive sensors and λ being the wavelength of the impinging signals. In the same way, we have

$$\boldsymbol{R'}_s^{(k)}(\boldsymbol{\psi}) = \int_{-\pi/2}^{\pi/2}\rho(\theta,\boldsymbol{\psi})\boldsymbol{a}(\theta)\boldsymbol{a}^T(\theta)d\theta.$$

After algebraic manipulations as done in [17], we show that the normalized unconjugated noise-free covariance matrix $\boldsymbol{R'}_s^{(k)}(\boldsymbol{\psi}_k)$ can be written as:

$$\boldsymbol{R'}_s^{(k)}(\boldsymbol{\psi}_k) = \boldsymbol{a}(\bar{\theta}_k)\boldsymbol{a}^T(\bar{\theta}_k) \odot \boldsymbol{T}'(\boldsymbol{\psi}_k) = \boldsymbol{\Phi}(\bar{\theta}_k)\boldsymbol{T}'(\boldsymbol{\psi}_k)\boldsymbol{\Phi}^T(\bar{\theta}_k), \tag{19}$$

where $\boldsymbol{T}'(\boldsymbol{\psi}_k)$ is a $(L \times L)$ real-valued Hankel matrix. Depending on the nature of the sources' angular distribution, we prove using [18] the following expressions:

$$[\boldsymbol{T}']_{pl}^{\text{Gauss}}(\boldsymbol{\psi}_k) = \exp\left(-\frac{1}{2}\left(\tfrac{2(p+l-2)\pi d}{\lambda}\sigma_k\cos(\bar{\theta}_k)\right)^2\right), \tag{20}$$

$$[\boldsymbol{T}']_{pl}^{\text{Unif}}(\boldsymbol{\psi}_k) = \text{sinc}\left(\tfrac{2(p+l-2)\pi d}{\lambda}\sigma_k\cos(\bar{\theta}_k)\right). \tag{21}$$

Inserting (16) and (19) in (10) and (11), respectively, we obtain the following expressions for $\boldsymbol{R}_{xx}$ and $\boldsymbol{R'}_{xx}$:

$$\boldsymbol{R}_{xx} = \sum_{k=1}^{K}\sigma_{s_k}^2\boldsymbol{\Phi}(\bar{\theta}_k)\boldsymbol{T}(\boldsymbol{\psi}_k)\boldsymbol{\Phi}^H(\bar{\theta}_k) + \sigma_n^2\boldsymbol{I}_L, \tag{22}$$

$$\boldsymbol{R'}_{xx} = \sum_{k=1}^{K}\sigma_{s_k}^2 e^{j\phi_k}\gamma_k\boldsymbol{\Phi}(\bar{\theta}_k)\boldsymbol{T}'(\boldsymbol{\psi}_k)\boldsymbol{\Phi}^T(\bar{\theta}_k), \tag{23}$$

To derive the CRB of the underlying estimation problem, we define the unknown parameter vector as follows:

$$\boldsymbol{\upsilon} = \left[\bar{\boldsymbol{\theta}}^T, \boldsymbol{\sigma}^T, \boldsymbol{\beta}^T, \boldsymbol{\gamma}^T, \boldsymbol{\phi}^T, \sigma_n^2\right]^T = \left[\boldsymbol{\psi}^T, \boldsymbol{\xi}^T\right]^T, \tag{24}$$

in which $\boldsymbol{\psi} = \left[\bar{\boldsymbol{\theta}}^T, \boldsymbol{\sigma}^T\right]^T$ represents the angular parameters vector while $\boldsymbol{\xi} = \left[\boldsymbol{\beta}^T, \boldsymbol{\gamma}^T, \boldsymbol{\phi}^T, \sigma_n^2\right]^T$ contains the nuisance parameters. The vector $\bar{\boldsymbol{\theta}} = \left[\bar{\theta}_1, \ldots, \bar{\theta}_K\right]^T$, contains the unknown central DOAs of the ID sources to be estimated. Moreover, $\boldsymbol{\sigma} = [\sigma_1, \ldots, \sigma_K]^T$ is the vector of the standard deviations to be estimated as well. Besides, $\boldsymbol{\beta} = \left[\sigma_{s_1}^2, \ldots, \sigma_{s_K}^2\right]^T$ gathers the powers of the sources. Finally, $\boldsymbol{\gamma} = [\gamma_1, \ldots, \gamma_K]^T$ and $\boldsymbol{\phi} = [\phi_1, \ldots, \phi_K]^T$ gather their noncircularity rates and phases, respectively. The CRB of the unknown parameter vector, $\boldsymbol{\upsilon}$, is defined as follows:

$$\text{CRB}(\boldsymbol{\upsilon}) = \boldsymbol{I}_{\text{F}}^{-1}(\boldsymbol{\upsilon}), \tag{25}$$

in which $\boldsymbol{I}_{\text{F}}(\boldsymbol{\upsilon})$ is the Fisher information matrix (FIM) corresponding to the unknown parameter vector, $\boldsymbol{\upsilon}$. Since the snapshots of the extended vector $\widetilde{\boldsymbol{x}}(t)$ defined in (14) are mutually independent, then, from [14], the ijth entry of $\boldsymbol{I}_{\text{F}}(\boldsymbol{\upsilon})$ is given by:

$$(\boldsymbol{I}_{\text{F}})_{ij} = \tfrac{N}{2}\text{tr}\left(\frac{\partial\boldsymbol{R}_{\widetilde{x}\widetilde{x}}}{\partial\upsilon_i}\boldsymbol{R}_{\widetilde{x}\widetilde{x}}^{-1}\frac{\partial\boldsymbol{R}_{\widetilde{x}\widetilde{x}}}{\partial\upsilon_j}\boldsymbol{R}_{\widetilde{x}\widetilde{x}}^{-1}\right), \tag{26}$$

where

$$\frac{\partial\boldsymbol{R}_{\widetilde{x}\widetilde{x}}}{\partial\upsilon_i} = \begin{pmatrix} \frac{\partial\boldsymbol{R}_{xx}}{\partial\upsilon_i} & \frac{\partial\boldsymbol{R'}_{xx}}{\partial\upsilon_i} \\ \left(\frac{\partial\boldsymbol{R'}_{xx}}{\partial\upsilon_i}\right)^* & \left(\frac{\partial\boldsymbol{R}_{xx}}{\partial\upsilon_i}\right)^* \end{pmatrix}.$$

The partial derivatives of $\boldsymbol{R}_{xx}$ are given by:

$$\begin{aligned}
\frac{\partial\boldsymbol{R}_{xx}}{\partial\bar{\theta}_i} &= \sigma_{s_i}^2\left(\frac{\partial\boldsymbol{\Phi}}{\partial\bar{\theta}_i}\boldsymbol{T}\boldsymbol{\Phi}^H + \boldsymbol{\Phi}\frac{\partial\boldsymbol{T}}{\partial\bar{\theta}_i}\boldsymbol{\Phi}^H + \boldsymbol{\Phi}\boldsymbol{T}\frac{\partial\boldsymbol{\Phi}^H}{\partial\bar{\theta}_i}\right),\\
\frac{\partial\boldsymbol{R}_{xx}}{\partial\sigma_i} &= \sigma_{s_i}^2\boldsymbol{\Phi}\frac{\partial\boldsymbol{T}}{\partial\sigma_i}\boldsymbol{\Phi}^H,\\
\frac{\partial\boldsymbol{R}_{xx}}{\partial\sigma_{s_i}^2} &= \boldsymbol{\Phi}\boldsymbol{T}\boldsymbol{\Phi}^H,\\
\frac{\partial\boldsymbol{R}_{xx}}{\partial\sigma_n^2} &= \boldsymbol{I}_L,\\
\frac{\partial\boldsymbol{R}_{xx}}{\partial\gamma_i} &= \frac{\partial\boldsymbol{R}_{xx}}{\partial\phi_i} = \boldsymbol{0}_{L\times L}.
\end{aligned}$$

In addition, the partial derivatives of $\boldsymbol{R'}_{xx}$ are given by:

$$\begin{aligned}
\frac{\partial\boldsymbol{R'}_{xx}}{\partial\bar{\theta}_i} &= \sigma_{s_i}^2 e^{j\phi_i}\gamma_i\left(\frac{\partial\boldsymbol{\Phi}}{\partial\bar{\theta}_i}\boldsymbol{T}'\boldsymbol{\Phi}^T + \boldsymbol{\Phi}\frac{\partial\boldsymbol{T}'}{\partial\bar{\theta}_i}\boldsymbol{\Phi}^T + \boldsymbol{\Phi}\boldsymbol{T}'\frac{\partial\boldsymbol{\Phi}^T}{\partial\bar{\theta}_i}\right),\\
\frac{\partial\boldsymbol{R'}_{xx}}{\partial\sigma_i} &= \sigma_{s_i}^2 e^{j\phi_i}\gamma_i\boldsymbol{\Phi}\frac{\partial\boldsymbol{T}'}{\partial\sigma_i}\boldsymbol{\Phi}^T,\\
\frac{\partial\boldsymbol{R'}_{xx}}{\partial\sigma_{s_i}^2} &= e^{j\phi_i}\gamma_i\boldsymbol{\Phi}\boldsymbol{T}'\boldsymbol{\Phi}^T,\\
\frac{\partial\boldsymbol{R'}_{xx}}{\partial\sigma_n^2} &= \boldsymbol{0}_{L\times L},\\
\frac{\partial\boldsymbol{R'}_{xx}}{\partial\phi_i} &= j\gamma_i\frac{\partial\boldsymbol{R'}_{xx}}{\partial\gamma_i} = j\gamma_i\sigma_{s_i}^2 e^{j\phi_i}\boldsymbol{\Phi}\boldsymbol{T}'\boldsymbol{\Phi}^T.
\end{aligned}$$

Therefore, from (24), $\boldsymbol{I}_{\text{F}}(\boldsymbol{\upsilon})$ takes the following form:

$$\boldsymbol{I}_{\text{F}}(\boldsymbol{\upsilon}) = \begin{pmatrix} \boldsymbol{I}_{\text{F}_{\boldsymbol{\psi},\boldsymbol{\psi}}} & \boldsymbol{I}_{\text{F}_{\boldsymbol{\psi},\boldsymbol{\xi}}} \\ \boldsymbol{I}_{\text{F}_{\boldsymbol{\xi},\boldsymbol{\psi}}} & \boldsymbol{I}_{\text{F}_{\boldsymbol{\xi},\boldsymbol{\xi}}} \end{pmatrix},$$

where $\boldsymbol{I}_{\text{F}_{\boldsymbol{\psi},\boldsymbol{\psi}}}$ and $\boldsymbol{I}_{\text{F}_{\boldsymbol{\xi},\boldsymbol{\xi}}}$ are the $\boldsymbol{\psi}$- and the $\boldsymbol{\xi}$-blocks of the $\boldsymbol{I}_{\text{F}}(\boldsymbol{\upsilon})$. Moreover, $\boldsymbol{I}_{\text{F}_{\boldsymbol{\psi},\boldsymbol{\xi}}}$ and $\boldsymbol{I}_{\text{F}_{\boldsymbol{\xi},\boldsymbol{\psi}}}$ are the joint matrices of the vectors $\boldsymbol{\psi}$ and the $\boldsymbol{\xi}$. We are interested only in the $\boldsymbol{\psi}$-block of the CRB, which we denote by $\text{CRB}(\boldsymbol{\psi})$. Using the inversion of partitioned matrices Lemma [11], we obtain the following expression for $\text{CRB}(\boldsymbol{\psi})$:

$$\text{CRB}(\boldsymbol{\psi}) = \left(\boldsymbol{I}_{\text{F}_{\boldsymbol{\psi},\boldsymbol{\psi}}} - \boldsymbol{I}_{\text{F}_{\boldsymbol{\xi},\boldsymbol{\psi}}}^T\boldsymbol{I}_{\text{F}_{\boldsymbol{\xi},\boldsymbol{\xi}}}^{-1}\boldsymbol{I}_{\text{F}_{\boldsymbol{\xi},\boldsymbol{\psi}}}\right)^{-1}. \tag{27}$$

IV. Illustrative simulations

In this section, we present some graphical representations showing the CRB of the angular parameters derived assuming *noncircular* ID sources . This CRB will be compared to the CRB derived in [13] for *circular* ID sources [referred to hereafter as CRB^{cir}] and to the CRBs of the central DOA derived in [9] and [14] assuming point iid sources for both *circular*

and *noncircular* signals, respectively. In all simulations, we consider a uniform linear array of 6 sensors separated by half a wavelength. The number of snapshots is $N = 1000$.

We first consider two equipowered *noncircular* ID sources with identical noncircularity rate $\gamma = 1$ and noncircularity phases $\phi_1 = \pi/3$ and $\phi_2 = \pi/4$. The sources are located at central DOAs $\bar{\theta}_1 = 10°$ and $\bar{\theta}_2 = 30°$ with respective standard deviations $\sigma_1 = 3°$ and $\sigma_2 = 5°$. Figs. 1(a) and 1(b) show both $\log(\text{CRB}^{\text{noncir}})$ and $\log(\text{CRB}^{\text{cir}})$ of $\bar{\theta}_1$ and σ_1, respectively, as a function the SNR when the sources have: i) the same Gaussian angular distribution (i.e., GID) and ii) different angular distributions (the first source have a Uniform angular distribution (i.e., UID) and the second source is GID). We see from Figs. 1(a) and 1(b) that the CRBs

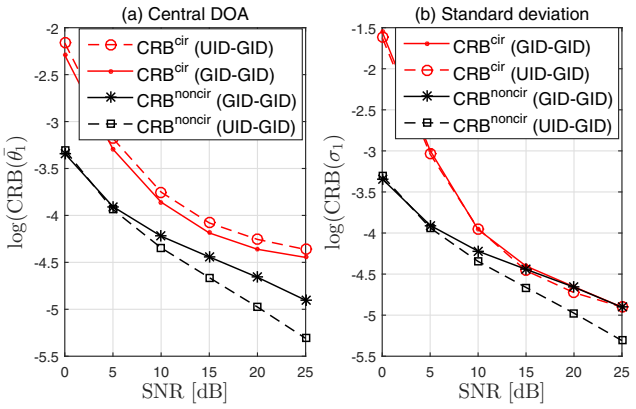

Figure 1. $\text{CRB}^{\text{noncir}}$ and CRB^{cir} of $\bar{\theta}_1$ and σ_1 versus the SNR in logarithmic scale.

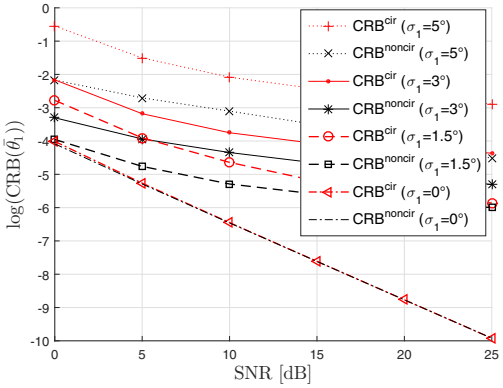

Figure 2. $\text{CRB}^{\text{noncir}}$ and CRB^{cir} of $\bar{\theta}_1$ versus the SNR in logarithmic scale for different values of σ_1.

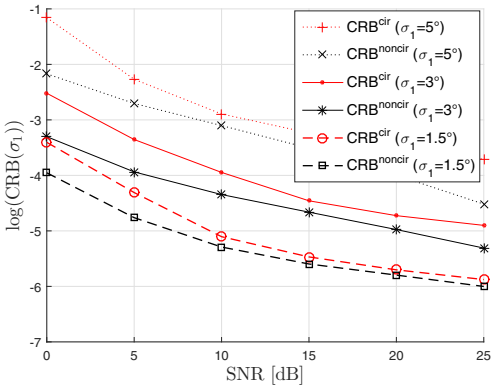

Figure 3. $\text{CRB}^{\text{noncir}}$ and CRB^{cir} of σ_1 versus the SNR in logarithmic scale for different values of σ_1.

obtained assuming *noncircular* ID sources are lower than those derived considering ID sources to be *circular*, especially for low SNR values. This illustrates the performance gain that the noncircularity offers to the estimation of the central DOAs as well as the angular spreads notably when the signals are very corrupted by the noise. We also show that the CRBs for the DOAs and the angular spreads depend on the form of the angular distribution of the sources. Moreover, it can be seen from these figures that the CRB^{cir} converges faster to the $\text{CRB}^{\text{noncir}}$, at high SNR, when the sources have the same angular distribution (GID-GID in our case). This means that for high SNR values, the noncircularity characteristic is more informative about the angular parameters when the sources have different distributions. Next, we study the influence of the angular spread on the angular parameters estimation by fixing σ_2 and varying σ_1. Thus, we reconsider two equipowered noncircular sources with different angular distributions (the first one is UID and the second one is GID). The standard deviation of the second source is fixed at $\sigma_2 = 3°$ while the standard deviation of the first source is varied from $\sigma_1 = 1.5°$ to $\sigma_1 = 3°$ and then to $\sigma_1 = 5°$. Figs. 2 and 3 show $\log(\text{CRB}^{\text{noncir}})$ and $\log(\text{CRB}^{\text{cir}})$ of $\bar{\theta}_1$ and σ_1, respectively, as a function of the SNR for the three values of σ_1. We also consider in Fig. 2 the case where both sources are point (i.e., non-distributed) corresponding to $\sigma_1 = \sigma_2 = 0$. We see from these figures that $\text{CRB}^{\text{noncir}}$ and CRB^{cir} increase as the angular spread increases and so does the difference between them. This can be explained by the fact that when σ increases, there is more room for the noncircularity of the signals to improve the angular parameters estimation performance. In fact, when σ increases, the signal becomes more dispersed and then the information provided by the noncircularity of the sources is more constructive in the estimation of the angular parameters. Now, to study the effect of the signals' noncircularity parameters (the noncircularity rate γ, the circularity phase separation $\Delta\phi$) on $\text{CRB}^{\text{noncir}}$ under different angular separations, $\Delta\theta$, we consider in Figs. 4(a), 4(b), 5(a) and 5(b) two ID sources. The first source is UID with central DOA fixed at $\bar{\theta}_1 = 10°$ and standard deviation $\sigma_1 = 3$ and the second one is GID with central DOA varied from $\theta_{02} = 18°$ to $\theta_{02} = 30°$ and standard deviation $\sigma_1 = 5$.

It can be seen from Figs. 5(a) and 5(b) that $\text{CRB}^{\text{noncir}}$ of the two angular parameters decreases as the noncircularity rate increases and this decrease is more prominent at low DOA separations. Moreover, it is seen that the difference between $\text{CRB}^{\text{noncir}}$ and CRB^{cir} increases as the DOA separation $\Delta\theta$ decreases. In fact, the ratio between the two CRBs tends to zero at low DOA separations (for $\Delta\theta = 8°$). Finally, from Fig. 5(a) and 5(b), we see that $\text{CRB}^{\text{noncir}}$ of the angular parameters is sensitive to the circularity phase separation especially at low DOA separations.

V. Conclusion

In this paper, we derived for the first time an explicit expression for the stochastic Cramér-Rao bounds (CRB) of the angular parameters estimates from ID signals generated

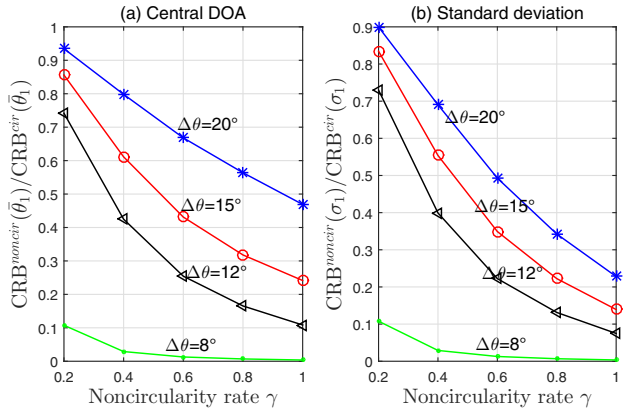

Figure 4. Ratio$(\bar{\theta}_1) = \left(\text{CRB}^{\text{noncir}}(\bar{\theta}_1)\right) / \left(\text{CRB}^{\text{cir}}(\bar{\theta}_1)\right)$ and Ratio$(\sigma_1) = \left(\text{CRB}^{\text{noncir}}(\sigma_1)\right) / \left(\text{CRB}^{\text{cir}}(\sigma_1)\right)$ as a function of the noncircularity rate γ for different values of DOA separation ($\Delta\theta$), for $\phi_1 = \pi/3$, $\phi_2 = \pi/4$, $N = 1000$ and $SNR = 5$ dB.

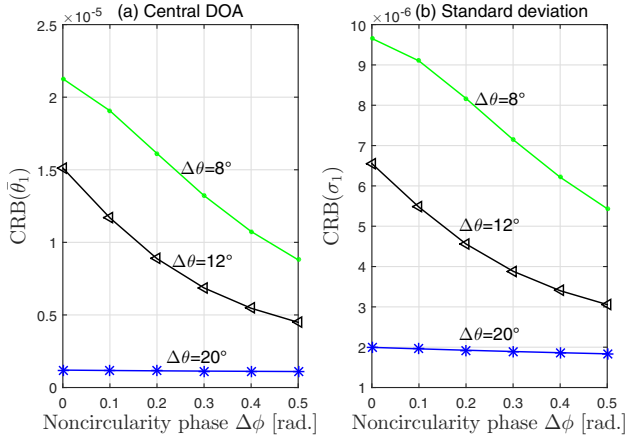

Figure 5. $\text{CRB}^{\text{noncir}}(\bar{\theta}_1)$ and $\text{CRB}^{\text{noncir}}(\sigma_1)$ as a function of the noncircularity phase $\Delta\phi$ for different values of DOA separation ($\Delta\theta$) for $\gamma = 1$, $N = 1000$ and $SNR = 5$ dB.

by *noncircular* sources. This CRB was compared to that for *circular* ID signals. The CRB of the DOAs estimates was also compared to that obtained for both *circular* and *noncircular* point sources. It was seen that the CRBs of the angular parameters obtained assuming *noncircular* ID sources are lower than those derived assuming *circular* and ID sources. This illustrates the potential gain that the noncircularity characteristic of the sources offers for the estimation of the angular parameters. Moreover, this gain is more prominent when the sources have different distributions and when the angular spread increases. Furthermore, the CRBs of the central DOAs estimates from point sources are lower than those obtained assuming ID sources. However, the noncircularity is more informative about the DOA estimates in the case of ID sources. Finally, the CRBs derived assuming *noncircular* ID signals depend on the noncircularity rate, the circularity phase separation and the DOA separation.

REFERENCES

[1] P. Stoica and A. Nehorai, "MUSIC, maximum likelihood, and Cramér-Rao bound: further results and comparisons," *IEEE Trans. Acoust., Speech, Sig. Process.*, vol. 38, no. 12, pp. 2140-2150, Dec. 1990.

[2] F. Haddadi, M.M. Nayebi, and M.R. Aref, "Direction-of-arrival estimation for temporally correlated narrowband signals," *IEEE Trans. Sig. Process.,* vol. 57, no. 2, pp. 600-609, Apr. 2009.

[3] S. Ben Hassen, F. Bellili, A. Samet and S. Affes, "DOA estimation of temporally and spatially correlated narrowband noncircular sources in spatially correlated white noise," *IEEE Trans. Sig. Process.,* vol. 59, no. 9, pp. 4108-4121, Sept. 2011.

[4] Y. Meng, P. Stoica, and K. M.Wong, "Estimation of the directions of arrival of spatially dispersed signals in array processing," *Proc. Inst. Elect. Eng.-Radar, Sonar Navigat.*, vol. 143, no. 1, pp. 1-9, Feb. 1996.

[5] P. Zetterberg, *Mobile cellular communications with base station antenna arrays: Spectrum efficiency, algorithms, and propagation models*, Ph.D. dissertation, Royal Inst. Technol., Stockholm, Sweden, 1997.

[6] A. Hassanien, S. Shahbazpanahi, and A. B. Gershman, "A generalized Capon estimator for localization of multiple spread sources," *IEEE Trans. Sig. Process.*, vol. 52, no. 1, pp. 280-283, Jan. 2004.

[7] Sh. Shahbazpanahi, Sh. Valaee, and A. B. Gershman, "A Covariance fitting approach to parametric localization of multiple incoherently distributed sources," *IEEE Trans. Sig. Process.,* vol. 52, no. 3, Mar. 2004.

[8] A. Zoubir, Y. Wang, and P. Chargé, "Efficient subspace-based estimator for localization of multiple incoherently distributed sources," *IEEE Trans. Sig. Process.,* vol. 56, no. 2, pp. 532-542, Feb. 2008

[9] P. Stoica, A. G. Larsson, and A. B. Gershman, "The stochastic CRB for array processing: A textbook derivation," *IEEE Sig. Process. Lett.*, vol. 8, no. 5, pp. 148-150, May 2001.

[10] D. Slepian, "Estimation of signal parameters in the presence of noise," *Trans. IRE Prof. Group Inform. Theory PG IT-3*, vol. 3, no. 3, pp. 68-89, 1954.

[11] P. Stoica and R. Moses, *Introduction to spectral analysis. Upper Saddle River*, NJ: Prentice-Hall, 1997.

[12] M. Viberg, P. Stoica, and B. Ottersten "Array processing in correlated noise fields based on instrumental variables and subspace fitting," *IEEE Trans. Sig. Process.,* vol. 43, no. 5, pp. 1187-1199, May 1995.

[13] M. Ghogho, O. Besson, and A. Swami, "Estimation of directions of arrival of multiple scattered sources,"*IEEE Trans. Sig. Process.*, vol. 49, no. 11, pp. 2467-2480, Nov. 2001.

[14] J. P. Delmas and H. Abeida, "Stochastic Cramér-Rao bound for noncircular signals with application to DOA estimation," *IEEE Trans. Sig. Process.,* vol. 52, no. 11, pp. 3192-3199, Nov. 2004.

[15] S. Ben Hassen, F. Bellili, A. Samet and S. Affes, "Closed form expression for the Cramér-Rao lower bound for the DOA estimates from spatially and temporally correlated narrowband signals considering noncircular sources," *ComNet. Conf.,* pp. 1-7, Nov. 2010.

[16] M. Souden, S. Affes, and J. Benesty, "A Two-stage approach to estimate the angles of arrival and the angular spreads of locally scattered sources,"*IEEE Trans. Sig. Process.*, vol. 56, no. 5, pp. 1968-1983, May 2008.

[17] M. Bengtsson, *Antenna array signal processing for high rank models*, Ph.D. dissertation, Signals, Sensors, Syst. Dept., Royal Institute of Technology, Stockholm, Sweden, 1999.

[18] I. S. Gradshteyn and I. M. Ryzhik. *Table of integrals, series, and products. Academic Press*, Inc., 4 edition, 1980.